Journal of Microelectronics and Electronic Packaging (2024) **21**, 25–34
Copyright © International Microelectronics Assembly and Packaging Society
ISSN: 1551-4897

Flip-Chip-Based Dual-Polarized Antenna-on-Package Arrays for 5G mmWave Modules

Thi Huyen Le[1,*] and Ivan Ndip[1,2]

***Abstract*—In this article, we present and illustrate a flip-chip-based antenna-on-package (AoP) concept for the development of 5G mmWave massive MIMO antenna arrays and frontend modules. Unlike conventional Antenna-in-Package concepts, our concept provides the flexibility to choose suitable and separate layer stack-ups and packaging materials for enabling the antennas and the frontend components to meet their respective specifications. To illustrate this concept, we designed, fabricated, and measured novel dual-polarized broadband AoP arrays in the 39 GHz frequency band for 5G mmWave MIMO applications. The array consists of 16 identical stacked patch elements. Each single antenna possesses a driven patch, which is vertically stacked to a parasitic element to improve the antenna performance. It is excited by two orthogonal probe-feds for dual polarization. Furthermore, we designed and optimized antenna arrays together with the solder interconnects used for mounting the antennas onto the multilayered interposer. Our results show that these interconnects could cause up to about 0.5 dB reduction in the realized gain of the antenna array. The fabricated antenna arrays were measured from 33 to 41 GHz. A peak gain of approximately 16 dBi was measured. Excellent correlation was obtained between all the measurement and simulation results.**

***Keywords*—5G mmWave, antenna arrays, antenna measurement, base station, broad-band, dual-polarization, gain, radiation pattern**

Introduction

With the rapid development of mobile communication networks, the expected requirements for the fifth mobile communication generation (5G) have been increased. Above all, there is a need for higher data rates and channel capacity to support a wide range of emerging applications in various applications and industries. To meet these requirements, the millimeter wave (mmWave) frequency band has been designated to be used for 5G. However, using mmWave bands leads to additional challenges in the design and integration of 5G mmWave frontend modules. One of these challenges is caused by high free-space losses, multipath fading, and shadowing in high-frequency bands, which may severely degrade the transmission quality, especially when communication occurs over long distances. To overcome this challenge, high-performance systems are required for 5G mmWave applications. To realize such systems, two factors play very important roles. Firstly, advanced packaging solutions, which can meet five key requirements, namely high performance, scalability, reliability, miniaturization, and low-cost requirements, are required [1]. Secondly, high-gain antennas with broadband and multipolarized characteristics are also needed. The performance of these antennas depends predominantly on the packaging substrate used for fabricating the antennas, as well as the stack-up of metal and dielectric layers.

In most of the published literature, mmWave antennas are designed and integrated with frontend ICs on the same substrate. The antennas are integrated into the package (Antenna-in-Package, AiP). For example, antennas integrated into mold substrates of wafer-level packages as in [2, 3] (see Fig. 1), or silicon-based antennas with integrated air cavities in [4]. Although these packaging concepts enable system miniaturization, they provide no flexibility in choosing packaging stack-up and material suitable for enabling the antennas and other system components to meet the specified requirements. This significantly limits the performance of the entire 5G mmWave module.

In this work, we present a flip-chip-based AoP packaging concept and substrate stack-up that provide flexibility to choose suitable and separate stack-ups and materials for enabling the antennas and other frontend components to meet their respective specifications. Unlike conventional approaches, the antennas in our proposed concept are integrated into the package (Antenna-on-Package, AoP). To illustrate this concept, we designed and fabricated novel dual-polarized broadband AoP arrays for 5G mmWave MIMO applications. One of the challenges of the AoP concept is the interconnect between the antenna and the package which may cause impedance mismatch and undesired reflections. In this work, we designed and optimized these interconnects, and thus enhanced the matching efficiency and gain of the antenna. The fabricated antennas were measured from 33 to 42 GHz. Excellent correlation is obtained between measurement and simulation results.

The present work is based on our contribution in [5], where a 2×2 antenna array was presented. In this article, we significantly expand on the design, analysis, fabrication, and measurement of the antennas presented in [5]. We extend the antenna array to a 4×4 dual-polarized broadband MIMO array and rigorously investigate different antenna parameters such as return loss, polarization, and mutual couplings between array elements. Furthermore, the radiation and beam scanning of the array are investigated and verified. Finally, we designed and optimized the 4×4 antenna array together with the antenna-to-package interconnect.

The rest of the article is structured as follows: In the section "Flip-Chip Based AoP Packaging Concept", the flip-chip-based

The manuscript was received on February 26, 2024; revision received on May 10, 2024; accepted on May 10, 2024.

[1]Fraunhofer Institute for Reliability and Microintegration, IZM, Gustav-Meyer-Allee 25, Berlin 13355, Germany

[2]Brandenburg University of Technology (BTU) Cottbus-Senftenberg, Platz der Deutschen Einheit 1, Konrad-Wachsmann-Allee 13, 03046 Cottbus, Germany

*Corresponding author; email: thi.huyen.le@izm.fraunhofer.de

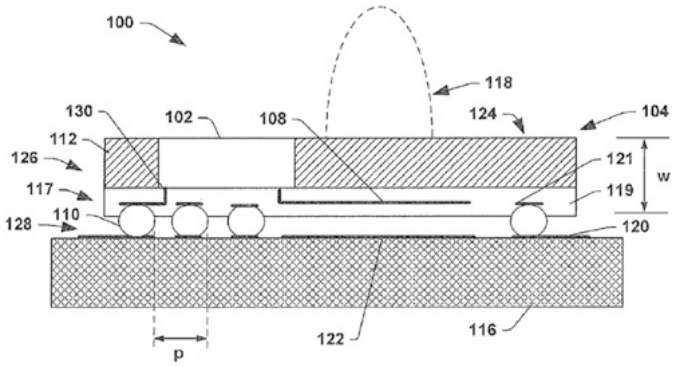

Fig. 1. Integrated antennas on wafer level package [2].

AoP packaging stack-up with the integrated antenna module is presented. In the section "5G mmWave AoP MIMO Antenna Array", the design and analysis of the dual-polarized antenna modules are extensively discussed. The fabrication and measurement as well as correlation between measurement and simulation results are shown in the section "Measurement Results".

Flip-Chip-Based AoP Packaging Concept

Fig. 2 shows our flip-chip-based AoP packaging concept with integrated antennas for mmWave applications.

The package consists of an antenna module, which is assembled onto a multilayered stack-up interposer, used for the integration of frontend ICs and passive components. The layer stack-ups and materials of the antenna module and the interposer can be chosen completely independent of each other to enable each of these modules to reach their respective specifications. This ensures both performance and cost optimization of the 5G mmWave module. For example, in this work, the antenna module consists of three metal and two dielectric layers, whereas the interposer module consists of four metal layers (two signal layers, and a power/ground plane pair) and three dielectric layers. Furthermore, the separate antenna module offers additional flexibility in testing before assembly onto the multilayered interposer as well as easy replacement, if necessary. To simplify the assembly process, the frontend ICs are also surface-mounted onto the interposer using flip-chip technology, just as the antenna. In comparison with other chip interconnection methods flip-chip technology provides shorter interconnects with smaller geometrical discontinuities, hence better antenna performance and signal integrity. The multilayered interposer, with the integrated antenna module and frontend components, can then be assembled on a system board using ball grid array (BGA) interconnects to enable system functionality.

5G mmWave AoP MIMO Antenna Array

A. Antenna Concept

In addition to the high-gain requirement, three additional antenna requirements for 5G mmWave modules are large bandwidth, polarization diversity, and MIMO. In the following sections, we will present the state-of-the-art antennas for 5G mmWave regarding these requirements, their limitations and our contribution that goes beyond state of the art.

Typically, microstrip antennas are often used for the development of wireless communication systems, because of their compactness, low cost, established fabrication techniques, and high integration density. However, the narrow bandwidth nature of these antennas limits their application in 5G mmWave mobile communications. To make microstrip patch antennas suitable for 5G mmWave applications, various techniques have been proposed to increase their bandwidth, e.g., using stacked patches [6] or U-slots configurations [7].

The polarization diversity of 5G mmWave antennas is desired for increasing the channel capacity without adding an additional antenna. This enables a reduction of installation space and, thus ensures low installation cost. Furthermore, dual-polarized antennas can help to reduce the polarization mismatch and are very useful in mitigating the multipath fading. Examples of dual-polarized antennas for 5G mmWave have been published in [8-20].

For the development of high-power modules for 5G mmWave applications such as base stations, (massive) MIMO antenna systems are required. Recently, some published works have focused on the design, investigation, and testing of 5G mmWave (massive) MIMO antenna arrays, which can be categorized in a single-band single-polarized configuration such as in [21-26], dual-band single-polarized configuration in [27], and single-band dual-polarized configuration in [28-31]. However, in most of these works, the specified 3 GHz bandwidth requirement was

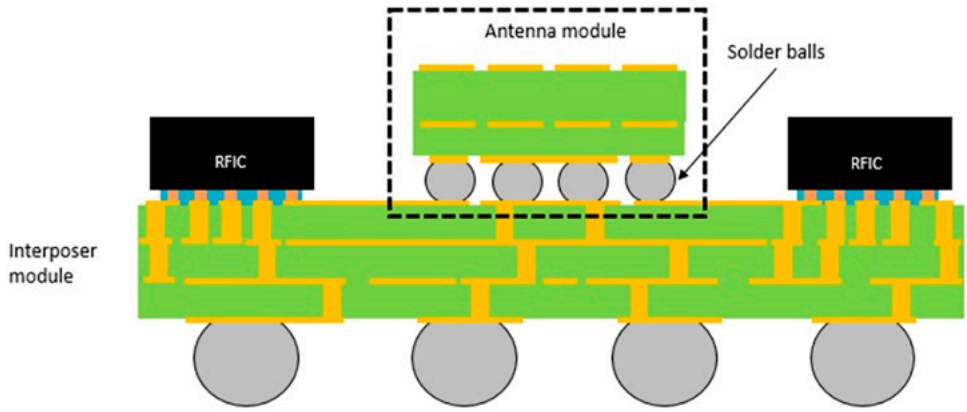

Fig. 2. Proposed flip-chip-based packaging concept with integrated antennas.

not fulfilled. In addition, the mutual coupling between array elements was not investigated. Most of the published works also rely on simulation results with no experimental validation.

In this work, we designed, analyzed, fabricated, and measured dual-polarized, broadband 4 × 4 MIMO antenna arrays, which can cover the entire specified 39 GHz frequency band of 5G mmWave and provide high gain, low polarization and mutual couplings between array elements. In addition, the beam steering of the array is also investigated. Our proposed 4 × 4 MIMO AoP, which meets all the specifications of a 5G mmWave antenna, can be up-scaled to obtain a massive MIMO antenna system. It can then be integrated into the multilayered interposer to develop a complete massive MIMO 5G mmWave system for base station applications.

In Fig. 3 our proposed 4 × 4 dual-polarized stacked microstrip patch antenna array having dimensions of 19 × 19 mm is shown. The array consists of 16 identical stacked patch elements, spaced by 4.5 mm to each other and excited by two orthogonal probe-feds for dual polarization.

Based on our proposed flip-chip-based AoP packaging concept in the section "Flip-Chip Based AoP Packaging Concept", a stack-up for design and demonstrator of the 4 × 4 dual-polarized MIMO antenna array is derived (see Fig. 4).

One of the key parameters in the design and optimization process of the antenna is to choose suitable combinations of substrate thicknesses for driven and parasitic patches in such a way, that two neighboring resonance frequencies are excited and properly coupled to achieve the required wide impedance bandwidth. For this purpose, possible combinations were investigated considering three criteria: (1) achieving the specified 3 GHz bandwidth, (2) having total thickness as small as possible for a high integration degree, (3) compliance with design rules of vias, pads for vias and BGA balls for later assembly onto the interposer module. The investigation results showed that a thickness combination of 300 and 127 µm meets all three criteria and is thus chosen for the antenna design. Therefore, the applied antenna stack-up consists of two PCB Astra MT77 substrate layers (ε_r = 3 and tanδ = 0.0017) with a top layer thickness of 300 µm, bottom layer thickness of 127 µm, and three copper layers (L1-L3), each having a thickness of 18 µm. Layer L1 includes the parasitic patch element, which is vertically stacked to the driven patch in layer L2, fed by two orthogonal probe-feds.

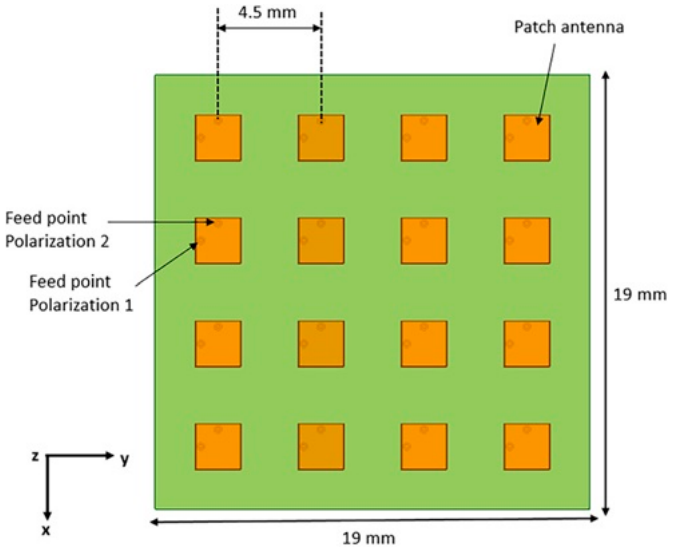

Fig. 3. Concept of the proposed 4 × 4 dual-polarized stacked patch MIMO antenna array.

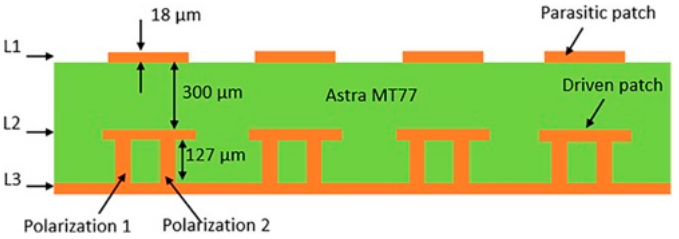

Fig. 4. Stack-up of the proposed 4 × 4 dual-polarized MIMO antenna array.

B. Antenna Module and Electromagnetic Simulation

Fig. 5 shows the simulation model of our proposed 4 × 4 dual-polarized stacked patch antenna array.

It consists of 16 identical stacked patch elements spaced by 4.5 mm to each other and has a total of 32 excitation ports. Each antenna possesses a driven patch, which is vertically stacked to a parasitic patch. The driven patch is excited by two orthogonal probe-feds to get the dual polarization characteristic. The parasitic patch is excited by the magnetic coupling of the driven patch and thus generates a second resonance frequency, which is close to the main resonance of the driven element. Due to a selection of suitable antenna substrate thicknesses and optimized design of the patch elements, these resonances are coupled to achieve a wide impedance bandwidth. The driven patch has square dimensions of 2.02 mm, whereas

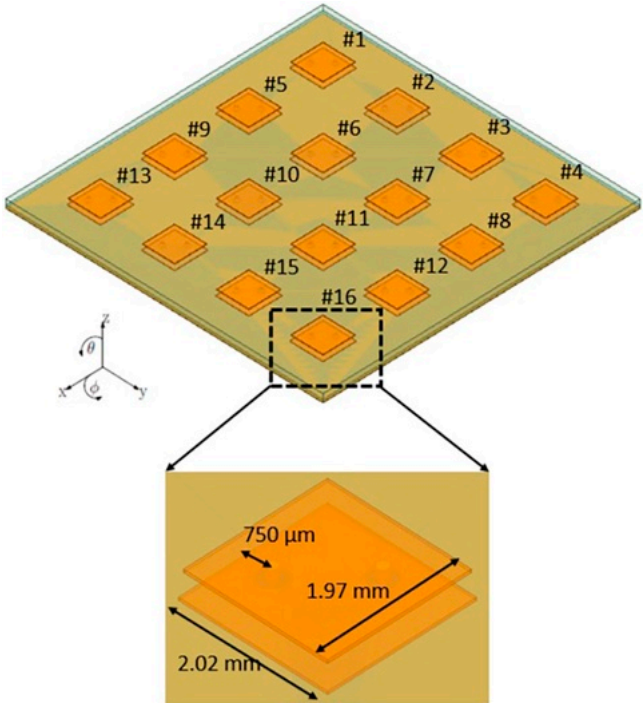

Fig. 5. Simulated MIMO 4 × 4 wide band dual-polarized stacked patch antenna array.

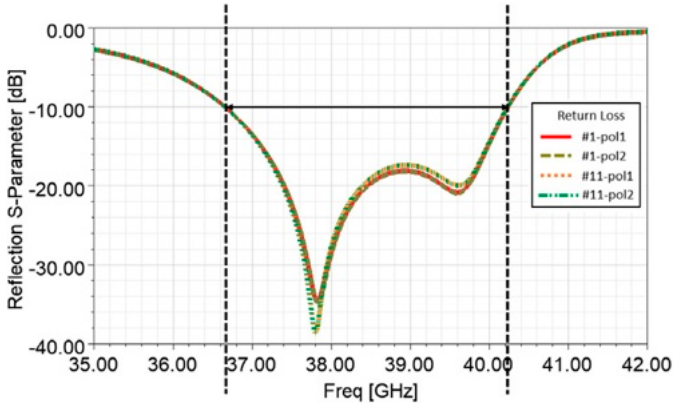

Fig. 6. Simulated return loss of the proposed 4 × 4 dual-polarized MIMO antenna array.

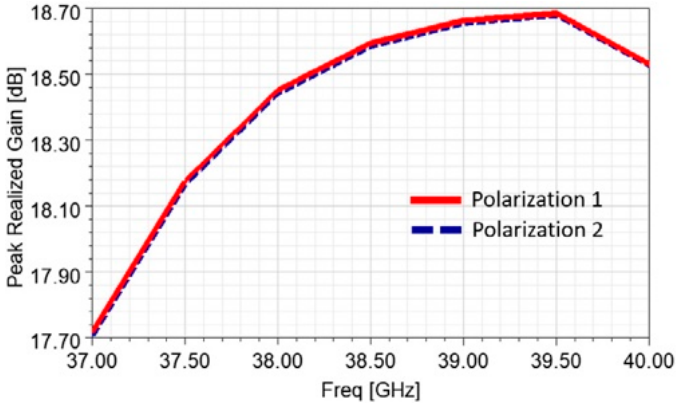

Fig. 8. Simulated peak realized gain over frequency of the proposed 4 × 4 dual-polarized MIMO antenna array.

the parasitic element has square dimensions of 1.97 mm. For modeling and simulation of the proposed antenna structure, ANSYS 3-D full-wave simulator (HFSS) was used. The simulations were performed from 35 to 42 GHz. Wave ports and radiation boundary conditions were used for the simulations. Fig. 6 shows the simulated return loss of patch element #1 for both polarizations in the proposed 4 × 4 antenna array. Since all array elements are identical, the other patch elements should have similar return loss characteristics like the first element. For example, in this figure, the return losses of element #11 are also plotted. The results show a simulated impedance bandwidth of 3.6 GHz (36.7 to 40.3 GHz) for both polarizations, which covers the entire specified 5G mmWave in the 39 GHz frequency band.

In Fig. 7 different couplings of the patch elements in the array are plotted. In the achieved bandwidth, the polarization coupling is lower than −20 dB, whereas the mutual couplings between array elements of less than −18 dB are achieved.

Fig. 8 shows the simulated peak realized gain of the 4 × 4 MIMO dual-polarized antenna array over the frequency range from 37 to 40 GHz. A peak gain between 17.7 and 18.7 dBi is achieved throughout the specified 39 GHz frequency band. The simulated radiation patterns in E- and H-plane at 38.5 GHz are shown in Fig. 9a for polarization 1 and in Fig. 9b for polarization 2. A very high peak gain of 18.6 dBi with a half-power beam width of 19° is achieved. The results show a side-lobe suppression of 13.2 dB. The proposed array has a radiation efficiency of 99.4%.

In Fig. 10, the beam steering from −40° to +40° of the array is shown for progressive phase shifts $\Delta\varphi_S$ of −150°, −75°, 0°, +75°, and +150° for polarization 1 (along X axis) and polarization 2 (along Y axis), which are determined based on eq. (1) and simulation technique.

$$\Delta\varphi_S = 360^\circ \times \frac{d_{\text{array}}}{\lambda} \times \sin\theta_S \tag{1}$$

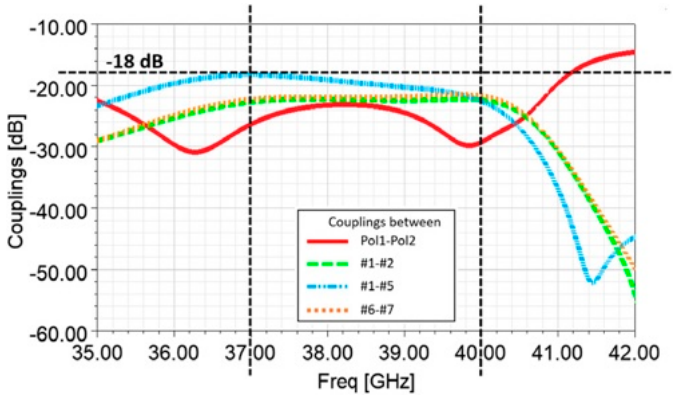

Fig. 7. Simulated couplings of the proposed 4 × 4 dual-polarized MIMO antenna array.

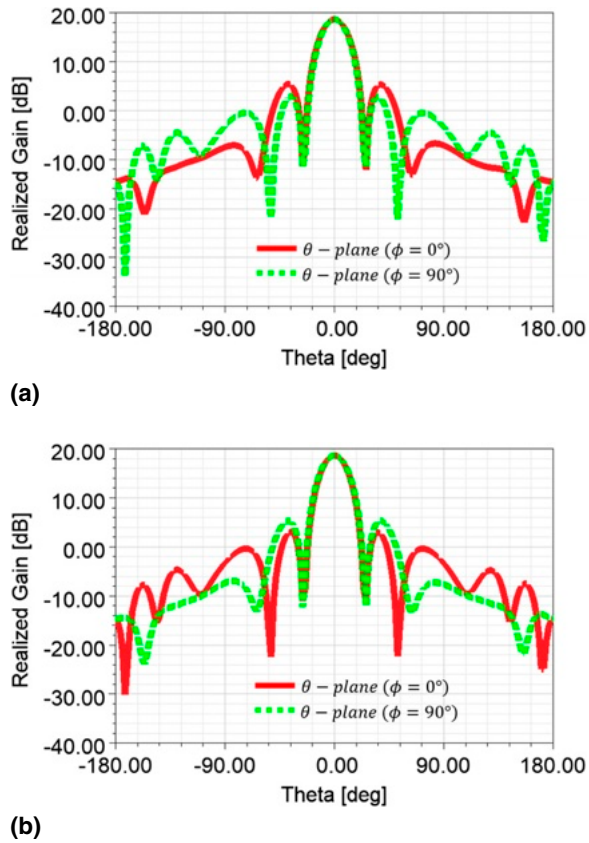

Fig. 9. Simulated radiation patterns of the proposed 4 × 4 dual-polarized MIMO antenna array: (a) polarization 1 and (b) polarization 2.

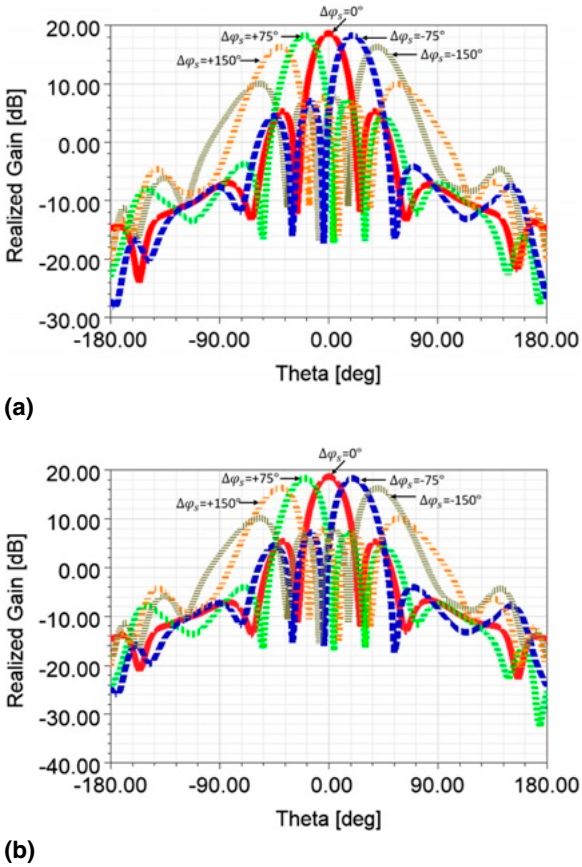

Fig. 10. Beam steering between −40° and +40° of the proposed 4 × 4 dual-polarized MIMO antenna array: (a) polarization 1 and (b) polarization 2.

where $\Delta\varphi_S$ is the progressive phase shift between array elements, d_{array} is the distance between array elements, λ is the wavelength at 39 GHz in free space, and θ_S is the scan angle in θ-plane. In this beam steering span, a maximum gain drop of 2.3 dBi and a maximum side-lobe of 10 dB are reached. In addition, the half-power beam width of the array is increased from 21.7° at 0° to about 26.5°/26.2° at −40°/+40°. In Table I, the values of important antenna parameters of the array at different scan angles are given.

The simulated results reveal that the proposed dual-polarized 4 × 4 antenna array with wide bandwidth, low couplings, high gain can meet the specifications for 5G mmWave applications.

Table I
Antenna Parameter at Different Scan Angles of the 4 × 4 Dual-Polarized MIMO Antenna Array

Scan angle [°]	Peak realized gain [dBi]	−3 dB Beamwidth [°]	Side-lobe suppression [dB]
−40	16.3	26.5	6.3
−20	18.2	23.2	11.2
0	18.6	21.7	13.2
+20	18.2	23.1	11.1
+40	16.2	26.2	6.2

C. Antenna Module with Solder Ball Interconnects

In this section, we model, simulate, and analyze the antenna module, considering the solder ball interconnects used for mounting the antenna onto the interposer. For these simulations, solder balls with a ball pitch of 750 µm, a ball diameter of 330 µm, and a height of 215 µm were chosen, as example, and arranged, as shown in Fig. 11. To evaluate the impact of the balls on the antenna performance, the antenna module is attached using the solder ball interconnects to the top layer of the interposer module, which consists of a single layer Astra MT77 with a thickness of 127 µm.

Fig. 12 shows the return loss of the antenna module with the solder interconnects. A simulated impedance bandwidth of about 3.6 GHz is achieved for all antenna elements and polarizations, because of identity and symmetry in the array.

In Fig. 13, the comparison of the peak realized gain over the frequency range between 37 and 40 GHz of the antenna array with and without solder ball interconnects is plotted. It can be seen that these interconnects cause a loss of approximately 0.3-0.5 dB. The radiation efficiency of the array reduces from 99% without solder ball interconnects to 95% with these interconnects.

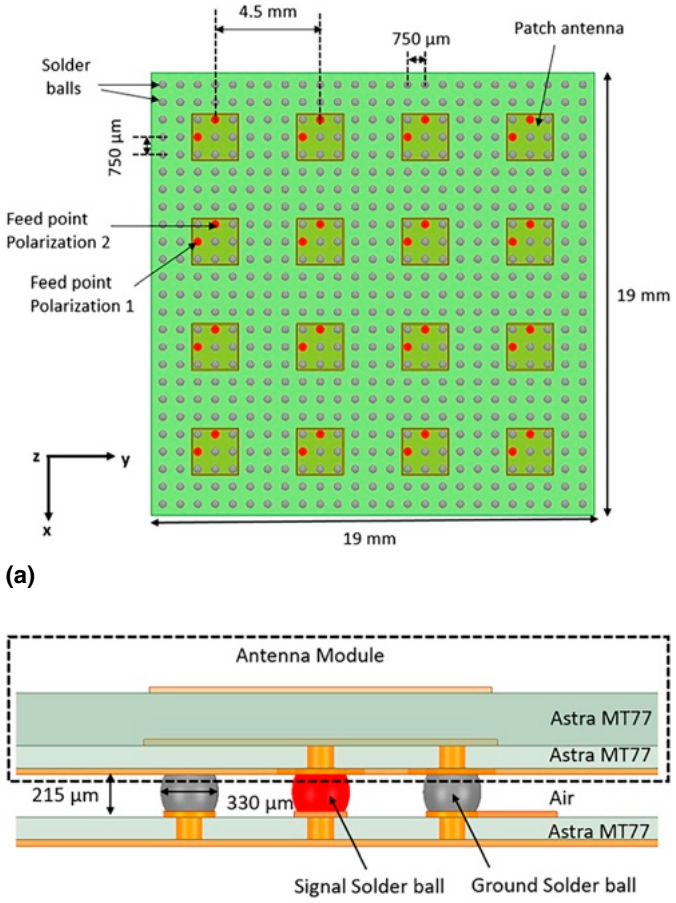

Fig. 11. The proposed 4 × 4 dual-polarized antenna array module with solder ball interconnects: (a) top view and (b) side view.

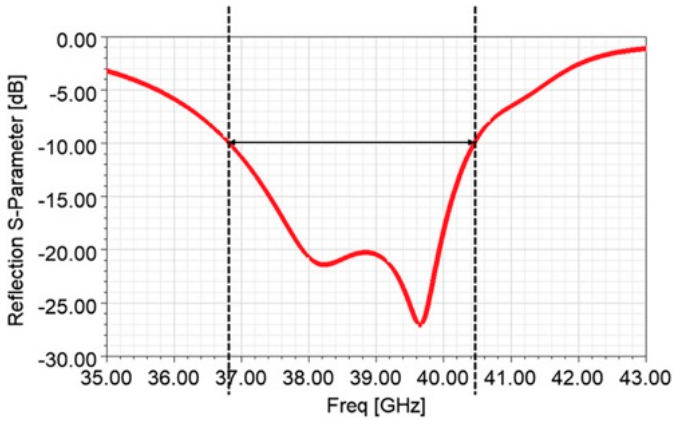

Fig. 12. Simulated return loss of the proposed 4 × 4 MIMO dual-polarized antenna array with solder ball interconnects.

In Figs. 14a and 14b, the radiation patterns at 38.5 GHz in the E- and H-plane of the array with the solder interconnects are shown for both polarizations.

Measurement Results

A. 2 × 2 Antenna Array

For verification of return loss, polarization, and mutual couplings between array elements, as well as radiation of a single antenna in the array, 2 × 2 dual-polarized antenna arrays with separate excitations were fabricated and measured. Fig. 15 shows an example of the fabricated 2 × 2 dual-polarized stacked patch antenna array with eight excitation ports for two linear polarizations, which has a size of 46 × 46 mm. To have enough place for the soldering of eight connectors for eight ports in the same board, the feed traces could not be identical. However, these feed lines were designed with the same optimized total physical length and width, so that all antenna ports can have approximately the same bandwidth, return loss, and phase.

Initially, the geometrical dimensions of the structures were measured with the aid of a microscope to capture any variations with respect to the design values. The results show a maximum fabrication tolerance in the antenna geometry of 30 μm.

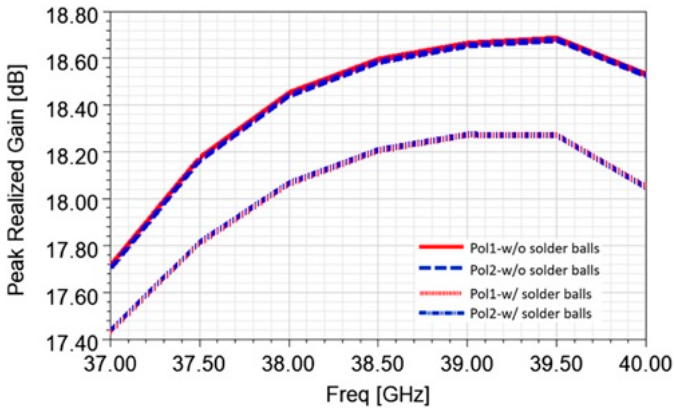

Fig. 13. Simulated peak realized gain over frequency of the proposed 4 × 4 MIMO dual-polarized antenna array with solder ball interconnects.

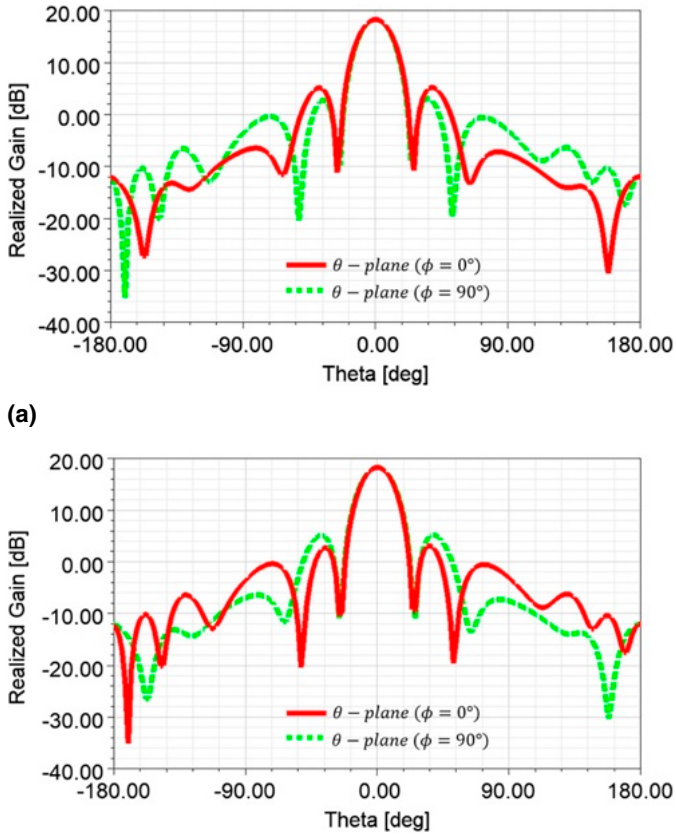

Fig. 14. Simulated radiation patterns of the proposed 4 × 4 MIMO dual-polarized antenna array with solder ball interconnects: (a) polarization 1 and (b) polarization 2.

Then, the scattering parameters and radiation characteristics of the fabricated 2 × 2 antenna array were measured with the aid of a coaxial connector (19S102-40 ML5) and Agilent's PNA network analyzer E8361A. The measurements were carried out inside an anechoic chamber (see Fig. 16).

The measured dimensions of the antenna were used to perform new antenna simulations. Fig. 17 shows a comparison between simulated and measured return loss of the single antenna in the array. A measured impedance bandwidth of 4.2 GHz (34.8 to 39 GHz) for port 1 and 3.9 GHz (34.9 to 38.8 GHz) for port 2 was achieved, whereas the simulated antenna bandwidth is 3.6 GHz. The isolation between two ports is lower than −20 dB in the achieved bandwidth (see Fig. 18).

Fig. 19 shows the simulated and measured peak realized gain of the single antenna element over the frequency range from 35 to 39 GHz. The measured antenna peak gain is about 6.5 dBi for port 1 and 6.6 dBi for port 2 compared with the simulated gain of 6.9 dBi.

In Figs. 20 and 21, the simulated and measured radiation patterns of the single array element in E- and H-plane for both polarizations are plotted. A radiation efficiency of about 81% is achieved. The mutual couplings between the antenna elements in the array are also measured. Fig. 22 shows that all couplings in the achieved antenna bandwidth are less than −20 dB.

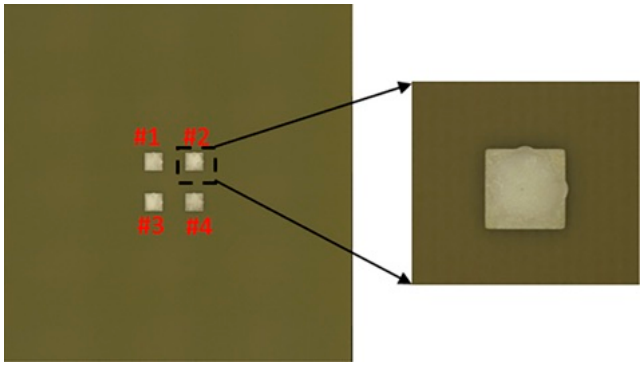

(a)

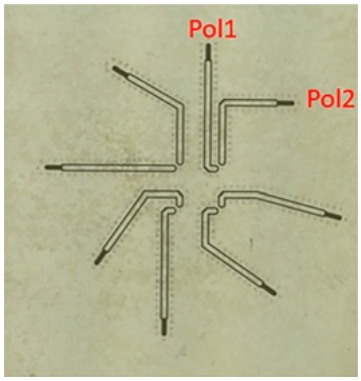

(b)

Fig. 15. Fabricated wide band dual-polarized stacked patch antenna array: (a) top view and (b) bottom view.

For the purpose of verification of the total gain, which the proposed antenna module can achieve, all antenna elements in the following 2 × 2 and 4 × 4 antenna arrays were fed together by using feeding networks. The simulated and measured results from the single antenna element show that both polarizations achieve similar results (as can be seen in Figs. 19-21). Therefore, to reduce the complexity of routing all ports (up to 32 routing lines in a 4 × 4 dual-polarized array), the antenna arrays excited by the feeding network were designed, fabricated, and measured only for one polarization. The radiation characteristic in the second polarization should be similar because of the symmetric arrangement in the array. Fig. 23 shows the simulated and fabricated 2 × 2 array with the feeding network.

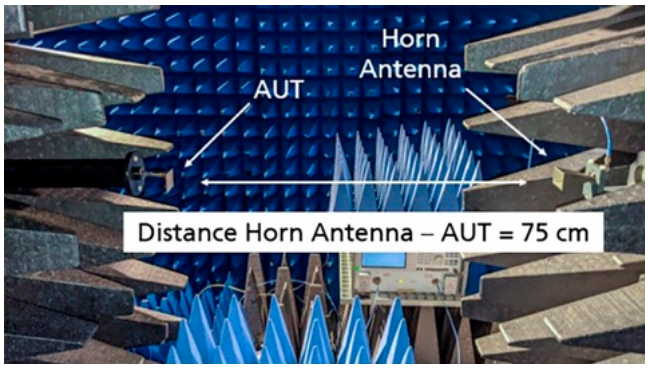

Fig. 16. Setup for the antenna radiation measurement.

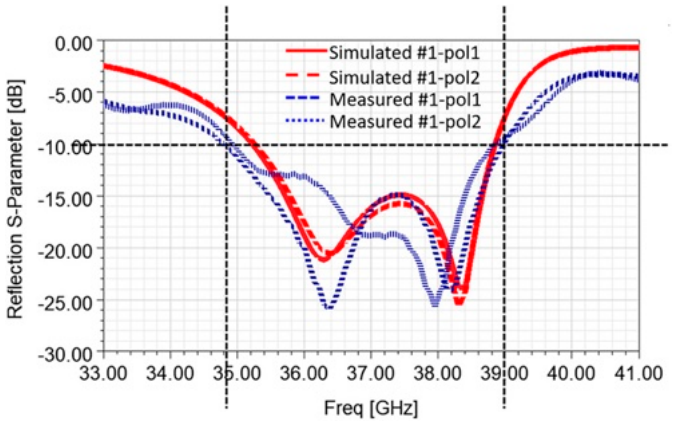

Fig. 17. Comparison between simulated and measured return loss (for both polarizations) of the dual-polarized single antenna.

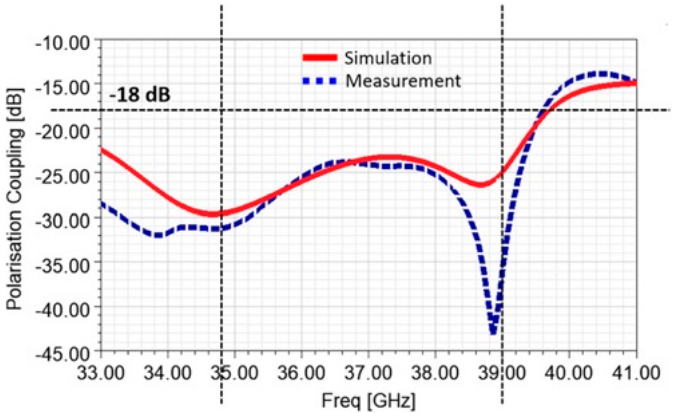

Fig. 18. Comparison between simulated and measured polarization couplings of the dual-polarized single antenna.

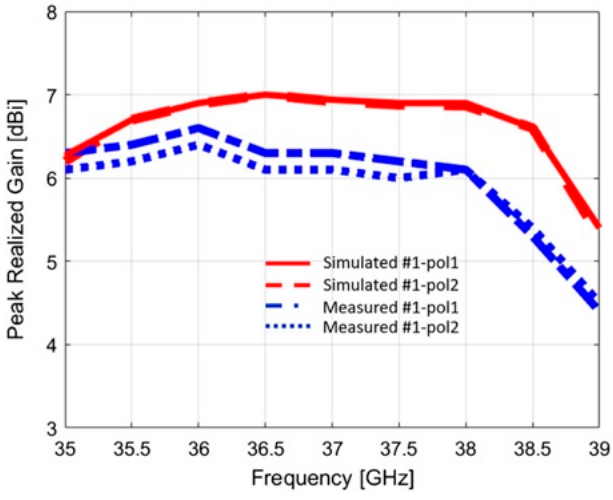

Fig. 19. Comparison between simulated and measured peak gain (for both polarizations) over the frequency of a dual-polarized single antenna.

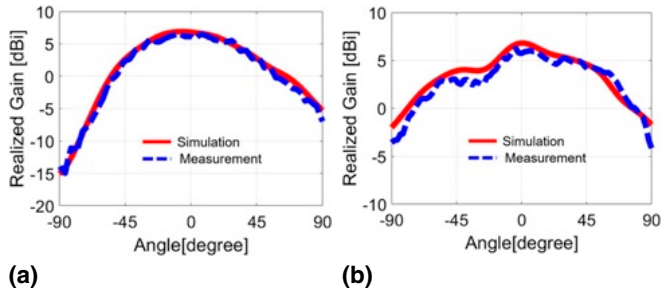

Fig. 20. Simulated and measured radiation pattern of polarization 1 of the proposed dual-polarized single antenna: (a) θ-Plane, ϕ = 0° and (b) θ-Plane, ϕ = 90°.

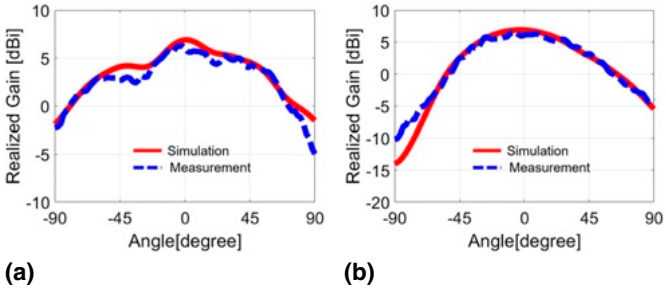

Fig. 21. Simulated and measured radiation pattern of polarization 2 of the proposed dual-polarized single antenna: (a) θ-Plane, ϕ = 0° and (b) θ-Plane, ϕ = 90°.

In Fig. 24, a comparison between simulated and measured return losses of this array is plotted. The measured reflection in the range between 37 and 39.5 GHz is lower than −10 dB.

Fig. 25 shows the simulated and measured radiation patterns in the E- and H-plane. A measured peak gain of 11.3 dBi and side-lobe suppression of 14.3 dB of the fabricated antenna are achieved, whereas the simulated structure has a peak gain of 11.5 dBi and side-lobe suppression of 15.4 dB. The radiation efficiency of the array is 83%.

B. 4 × 4 Antenna Array

Fig. 26 shows a simulated and fabricated 4 × 4 antenna array with a feeding network for exciting all array elements.

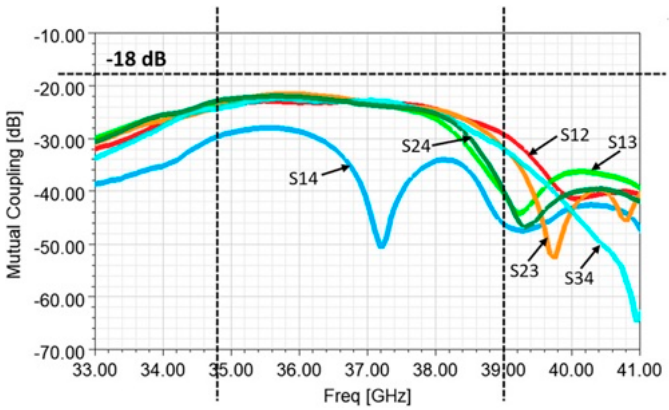

Fig. 22. Measured mutual couplings between antenna elements in the 2 × 2 dual-polarized antenna array.

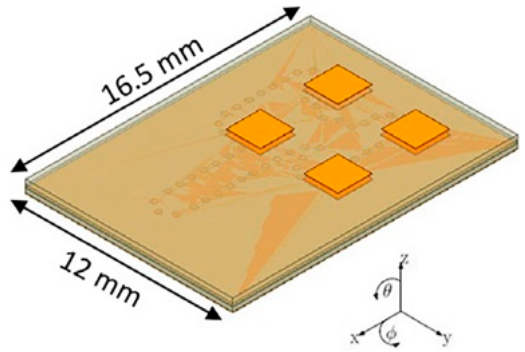

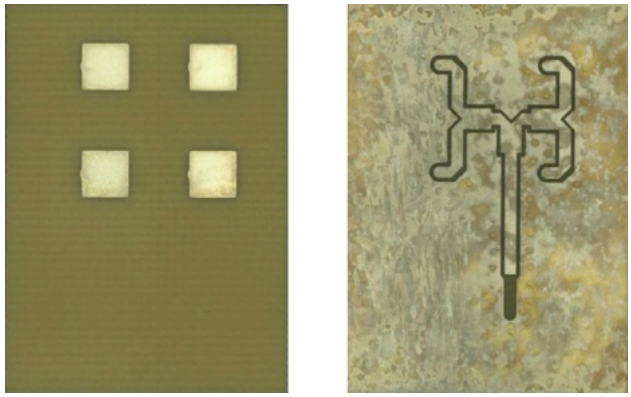

Fig. 23. Simulated and fabricated 2 × 2 antenna array with a corporate feeding network: (a) simulated and (b) fabricated: top (left) and bottom (right).

In Fig. 27 the measured return loss is compared with the simulated one. A very good correlation is obtained. The measured reflection in the range between 35.8 and 39.8 GHz is below −10 dB.

Fig. 28 shows the simulated and measured radiation patterns in the E- and H-plane. A maximum measured gain of 16 dBi with a side-lobe suppression of about 11.3 dB in the E-plane and 13 dB in the H-plane is achieved. The feeding network

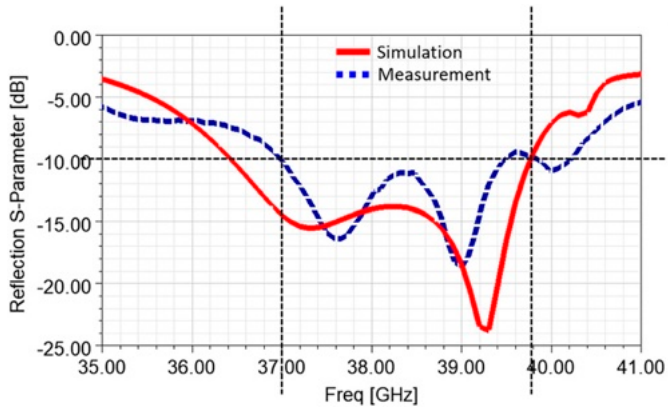

Fig. 24. Simulated and measured return loss of the 2 × 2 antenna array with a feeding network.

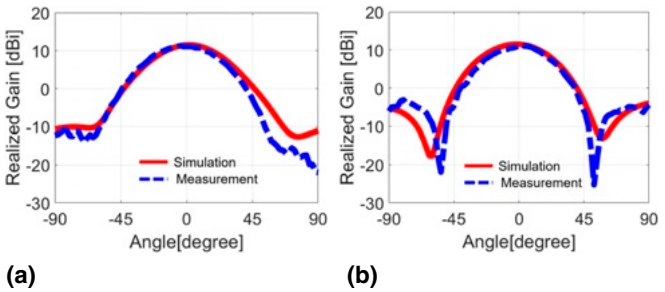

Fig. 25. Simulated and measured radiation pattern of the 2 × 2 antenna array with a feeding network: (a) θ-Plane, ϕ = 0° and (b) θ-Plane, ϕ = 90°.

causes a loss of approximately 2-3 dBi in the antenna gain. The radiation patterns show a measured half-power beam width of about 21° in the E-plane and H-plane. The radiation efficiency of the array is 81%.

Conclusions

In this work, a flip-chip-based AoP concept for 5G mmWave applications is presented and illustrated. It enables flexible choosing of suitable and separate stack-ups and materials for enabling the antennas and frontend components to meet their respective specifications. To illustrate this concept, novel dual-polarized broadband 4 × 4 MIMO antenna arrays were developed in the 39 GHz frequency band that can be mounted on a multilayered substrate on which the frontend components are assembled. The stacked patch method was used to improve the antenna performance. Two orthogonal probe-feds excite a single antenna element in the array for dual polarization. Furthermore, the impact of the solder ball interconnects used to assemble the antennas onto the multilayered interposer on antenna performance was also investigated. Our results show that these interconnects cause approximately 0.5 dB reduction in the realized gain of the antenna. The antenna arrays were fabricated using low-cost and high-performance PCB materials and measured from 33 to 41 GHz. Excellent correlation was obtained between measurement and simulation results. The results show very wide measured impedance bandwidths of approximately 4 GHz, which can cover the entire 39 GHz frequency band, and a high peak gain of 6.5 dBi of a single antenna for both polarizations. Low couplings of below −20 dB between two polarizations and array elements are measured in the achieved bandwidth. The 4 × 4 antenna array has a measured total peak gain of 16 dBi. The investigation shows a beam steering of the array between −40° and +40° with a maximum gain drop of about 2.3 dBi.

The results demonstrate that the proposed packaging concept and antenna array are very suitable for developing of 5G mmWave modules.

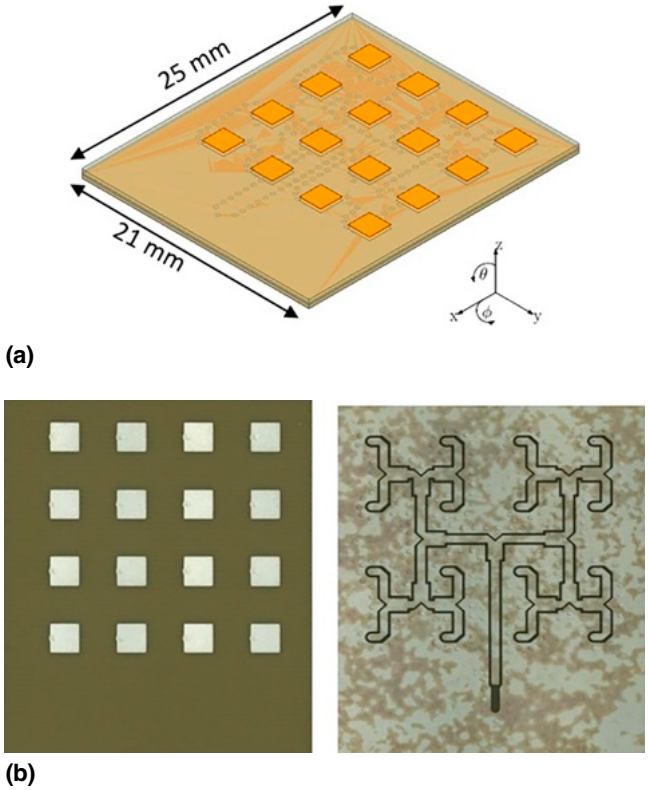

Fig. 26. Simulated and fabricated 4 × 4 antenna array with a corporate feeding network: (a) simulated and (b) fabricated: top (left) and bottom (right).

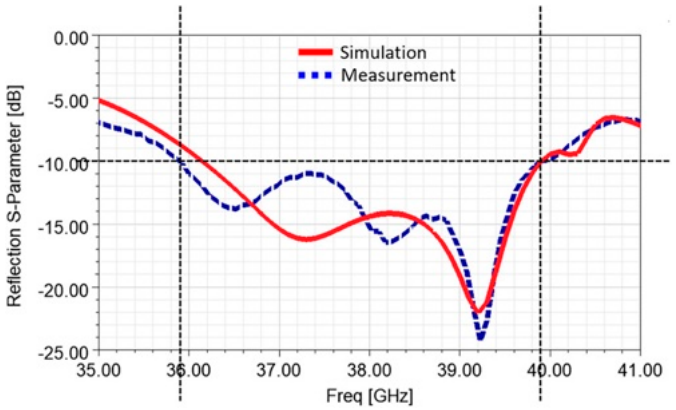

Fig. 27. Simulated and measured return loss of the 4 × 4 antenna array with a feeding network.

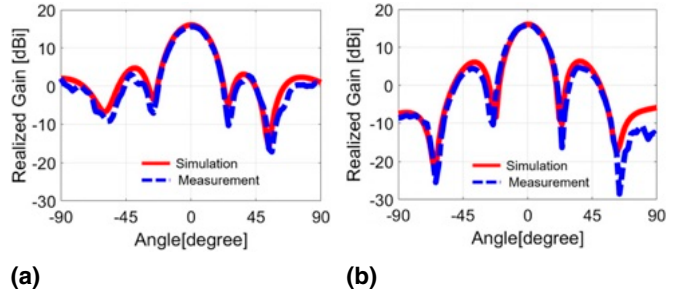

Fig. 28. Simulated and measured radiation pattern of the 4 × 4 antenna array with a feeding network: (a) θ-Plane, ϕ = 0° and (b) θ-Plane, ϕ = 90°.

Acknowledgments

The authors would like to thank Dr. Tekfouy Lim, Uwe Maass, and Michael Kaiser (Fraunhofer IZM) for supporting this work.

REFERENCES

[1] I. Ndip and K.-D. Lang, "Roles and requirements of electronic packaging in 5G," Proceedings of the 7th Electronic System Integration Technology Conference (ESTC), pp. 1-5, Dresden, Germany, 2018.

[2] R. Lachner, L. Maurer, and M. Wojnowski, "Integrated antennas in wafer level package," US Patent No. 20140117515A1, 1 May 2014.

[3] C.-H. Tsai, J. Hsieh, M. Liu, E. Yeh, H.-H. Chen, C.W. Hsiao, C.-S. Chen, C.-S. Liu, M. Lii, C.-T. Wang, and D.C.H. Yu, "Array antenna integrated fan-out wafer level packaging (in FOWLP) for millimeter wave system applications," Proceedings of the IEEE International Electron Devices Meeting (IEDM), pp. 25.1.1-25.1.4, Washington, DC, 2013.

[4] J.M. Cotte, B. P. Gaucher, J. Grzyb, N. D. Hoivik, C. V. Jahnes, J. U. Knickerbocker, D. Liu, J. H. Magerlein, C. S. Patel, U. R. Pfeiffer, C. K. Tsang, "Versatile Si-based packaging with integrated passive components for mmWave applications," US Patent No. 7,518,229, 14 April 2009.

[5] T.H. Le, O. Schwanitz, I. Ndip, T. Lim, U. Maaβ, M. Kaiser, and M. Schneider-Ramelow, "Wide band dual polarized antenna array for 5G mmWave based massive MIMO base station applications," Proceedings of the 24th International Microwave and Radar Conference (MIKON), pp. 1-4, Gdansk, Poland, 2022.

[6] B. Shi and C. Deng, "28/38 GHz single-feed stacked patch antenna for 5G communication," Proceedings of the International Conference on Microwave. Millimeter Wave Technology (ICMMT), pp. 1-3, Guangzhou, China, 2019.

[7] K. Keum and J. Choi, "A 28 GHz 4 × 4 U-slot patch array antenna for mm-wave communication," Proceedings of the International Symposium on Antennas and Propagation (ISAP), pp. 1-2, Busan, Korea (South), 2018.

[8] H.M. Santos, P. Pinho, and H.M. Salgado, "Dual-polarized patch antenna-in-package with high isolation for Ka-band 5G communications," Proceedings of the SBMO/IEEE MTT-S International Microwave Optoelectronics Conference (IMOC), pp. 1-3, Aveiro, Portugal, 2019.

[9] Y. Sun, S. Liao, W. Zhang, W. Che, and Q. Xue, "A compact dual-polarized stacked patch antenna for 5G millimeter-wave applications," Proceedings of the IEEE Asia-Pacific Microwave Conference (APMC), pp. 320-322, Hong Kong, Hong Kong, 2020.

[10] H. Xia, T. Zhang, L. Li, and F. Zheng, "A low-cost dual-polarized 28 GHz phased array antenna for 5G communications," Proceedings of the International Workshop Antenna Technology (iWAT), pp. 1-4, Nanjing, China, 2018.

[11] Y. Wang and D. Piao, "A compact size dual-polarized high-gain resonant cavity antenna at 28 GHz," Proceedings of the International Applied Computational Electromagnetics Society Symposium (ACES), pp. 1-2, Suzhou, China, 2017.

[12] I. Hwang, H. Jo, B.K. Ahn, J. Oh, and J. Yu, "Cavity-backed stacked patch array antenna with dual polarization for mmWave 5G base stations," Proceedings of the 13th European Conference on Antennas and Propagation (EuCAP), pp. 1-5, Krakow, Poland, 2019.

[13] S.S. Haider, F.A. Tahir, H.T. Chattha, and Q.H. Abbasi, "Compact polarization diversity antenna for 28/38 GHz bands," Proceedings of the 18th International Symposium on Antenna Technology and Applied Electromagnetics (ANTEM), pp. 1-2, Waterloo, ON, Canada, 2018.

[14] S.S. Haider, M.R. Wali, F.A. Tahir, and M.U. Khan, "A fractal dual- band polarization diversity antenna for 5G applications," Proceedings of the IEEE International Symposium on Antennas and Propagation and USNC/URSI National Radio Science Meeting, pp. 763-764, San Diego, CA, 2017.

[15] S. Lee, S. Kim, and J. Choi, "Dual-band dual-polarized proximity fed patch antenna for 28 GHz/39 GHz 5G millimeter-wave communications," Proceedings of the 13th European Conference on Antennas and Propagation (EuCAP), pp. 1-5, Krakow, Poland, 2019.

[16] Y. He, M. Rao, Y. Liu, G. Jing, M. Xi, and L. Zhao, "28/39-GHz dual-band dual-polarized millimeter wave stacked patch antenna array for 5G applications," Proceedings of the International Workshop on Antenna Technology (iWAT), pp. 1-4, Bucharest, Romania, 2020.

[17] M. Stanley, Y. Huang, H. Wang, H. Zhou, A. Alieldin, S.D. Joseph, C. Song, and T. Jia, "A dual-band dual-polarised stacked patch antenna for 28 GHz and 39 GHz 5G millimetre-wave communication," Proceedings of the 13th European Conference on Antennas and Propagation (EuCAP), pp. 1-4, Krakow, Poland, 2019.

[18] H. Lin and Y. Lin, "A dual-band and dual-polarized aperture antenna for 5G millmeter-wave applications," Proceedings of the IEEE International Symposium on Antennas and Propagation and USNC/URSI National Radio Science Meeting, pp. 423-424, Atlanta, GA, 2019.

[19] Z. Siddiqui, M. Sonkki, J. Chen, M. Berg, M.E. Leinonen, and A. Pärssinen, "Dual-band dual-polarized antenna for mm-wave 5G base station antenna array," Proceedings of the 14th European Conference on Antennas and Propagation (EuCAP), pp. 1-4, Copenhagen, Denmark, 2020.

[20] C. Chu, J. Zhu, S. Liao, A. Zhu, and Q. Xue, "28/38 GHz dual-band dual-polarized highly isolated antenna for 5G phased array applications," Proceedings of the IEEE MTT-S International Wireless Symposium (IWS), pp. 1-3, Guangzhou, China, 2019.

[21] S. Yamaguchi, H. Watanabe, H. Yoshioka, Y. Morimoto, H. Nakamizo, K. Tsutsumi, S. Shinjo, S. Uchida, A. Okazaki, T. Fukasawa, and N. Yoneda, "Development of 28GHz band massive MIMO antenna RF frontend module for 5G," Proceedings of the IEEE International Symposium on Antennas and Propagation and USNC/URSI National Radio Science Meeting, pp. 629-630, Boston, MA, 2018.

[22] M.K. Ishfaq, T.A. Rahman, Y. Yamada, and K. Sakakibara, "8 × 8 phased series fed patch antenna array at 28 GHz for 5G mobile base station antennas," Proceedings of the IEEE-APS Topical Conference on Antennas and Propagation Wireless Communications (APWC), pp. 160-162, Verona, Italy, 2017.

[23] T. Yuwono, M. Ismail, and I. Hajar, "Design of massive MIMO for 5G 28 GHZ," Proceedings of the 2nd International Conference on Computer Applications and Information Security (ICCAIS), pp. 1-4, Riyadh, Saudi Arabia, 2019.

[24] S. Krishna, G. Mishra, and S.K. Sharma, "A series fed planar microstrip patch array antenna with 1D beam steering for 5G spectrum massive MIMO applications," Proceedings of the IEEE Radio and Wireless Symposium (RWS), pp. 209-212, Anaheim, CA, 2018.

[25] L. Ren, B. Lu, F. Lu, and Y. Shu, "Modular and scalable millimeter-wave patch array antenna for 5G MIMO and beamforming," Proceedings of the 50th European Microwave Conference (EuMC), pp. 336-339, Utrecht, Netherlands, 2021.

[26] Y. Yin, S. Zihir, T. Kanar, and G.M. Rebeiz, "A 37-42 GHz 8 × 8 phased-array for 5G communication systems with 48-50 dBm EIRP," Proceedings of the IEEE MTT-S International Microwave Symposium (IMS), pp. 480-483, Boston, MA, 2019.

[27] M.M.M. Ali and A.-R. Sebak, "Design of compact millimeter wave massive MIMO dual-band (28/38 GHz) antenna array for future 5G communication systems," Proceedings of the 17th International Symposium on Antenna Technology and Applied Electromagnetics (ANTEM), pp. 1-2, Montreal, QC, Canada, 2016.

[28] S. Krishna and S.K. Sharma, "A dual polarization massive MIMO panel array antenna at Ka-band with beamforming capability," Proceedings of the United States National Committee of URSI National Radio Science Meeting (USNC-URSI NRSM), pp. 1-2, Boulder, CO, 2017.

[29] H. Xia, T. Zhang, L. Li, and F.-C. Zheng, "A low-cost dual-polarized 28 GHz phased array antenna for 5G communications," Proceedings of the International Workshop on Antenna Technology (iWAT), pp. 1-4, Nanjing, China, 2018.

[30] X. Gu, D. Liu, C. Baks, O. Tageman, B. Sadhu, J. Hallin, L. Rexberg, and A. Valdes, "A multilayer organic package with 64 dual-polarized antennas for 28GHz 5G communication," Proceedings of the IEEE MTT-S International Microwave Symposium (IMS), pp. 1899-1901, Honolulu, HI, 2017.

[31] D. Liu, X. Gu, C.W. Baks, and A. Valdes-Garcia, "Antenna-in-package design considerations for Ka-band 5G communication applications," *IEEE Transactions on Antennas and Propagation*, Vol. 65, No. 12, pp. 6372-6379.